

Large Scale Rapidity Correlations in Heavy Ion Collisions

Yuri V. Kovchegov¹, Eugene Levin^{1,2} and Larry McLerran¹

¹*Physics Department, Brookhaven National Laboratory
Upton, NY 11973, USA*

²*School of Physics and Astronomy, Tel Aviv University
Tel Aviv, 69978, Israel **

We discuss particle production mechanisms for heavy ion collisions. We present an argument demonstrating how the fluctuations of the number of produced particles in a series of classical emissions can account for KNO scaling. We predict rapidity correlations in the particle production in the event by event analysis of heavy ion collisions on the rapidity scales of the order of $1/\alpha_s$.

I. INTRODUCTION

In ultrarelativistic heavy ion collisions in the upcoming experiments at the Relativistic Heavy Ion Collider (RHIC) at Brookhaven and Large Hadron Collider (LHC) at CERN, a very high multiplicity of particles will be produced. Most of the models predict the multiplicities of produced hadrons per unit of rapidity in a given event to be of the order of [1]

$$\frac{dN}{dy} \sim 10^3, \quad (1)$$

where the exact number depends on the particular model. For these high multiplicities the scale of statistical fluctuations in one unit of rapidity is expected to be of the order of $\sigma \sim \sqrt{dN/dy}$ so that

$$\frac{\sigma}{dN/dy} \sim 10^{-1} - 10^{-2}. \quad (2)$$

Thus the multiplicities would not change much within each narrow bin in rapidity, as long as the number of particles produced in that rapidity bin is large. Collisions may therefore be studied on an event by event basis with little ambiguity. The fluctuations of multiplicities in each of the rapidity bins could be observed by examining several different events. One might wonder whether the numbers of particles produced in different rapidity bins are completely independent of each other, or there are certain correlations among them. In this paper we are going to address the question of rapidity correlations in the framework of McLerran–Venugopalan model of particle production by a series of classical emissions [2–6].

In McLerran–Venugopalan model [2] the high multiplicity per unit area gives rise to a dimensionfull parameter characterizing the nuclear collision

*Permanent address

$$\Lambda^2 = \frac{1}{\pi R^2} \frac{dN}{dy} \quad (3)$$

with R the nuclear radius. It was argued that this scale represents the typical transverse momentum of the particles produced in the early stages of the nuclear collisions [2,7]. Due to the high multiplicities of Eq. (1) this typical transverse momentum scale of produced partons given by Eq. (3) may become large compared to the QCD scale

$$\Lambda^2 \gg \Lambda_{QCD}^2. \quad (4)$$

The QCD coupling at the scale Λ is weak, $\alpha_s(\Lambda) \ll 1$. Together with the fact that the number of color charge sources in the nuclei is large this allows us to assume that the gluons produced in a nuclear collision could be described by the classical field of the colliding nuclei [2,3]. Here by classical field we mean that the gluon field is a solution of Yang–Mills equations of motion with the nuclei providing the source term for the equations [2–4]. A renormalization group (RG) approach has been developed recently to account for a series of classical emissions [5,6]. The procedure invented in [5,6] is the following: at each step of the evolution in rapidity each nucleus through classical emissions produces several partons with soft longitudinal momenta. At the next step of the RG the partons produced in the previous step are included in the source, off which the next generation of even softer partons is emitted. That way the produced soft partons modify the density of color sources, for which one writes a renormalization group equation [5,6]. The exact form of this equation is not important for our discussion here. We just note that at the lowest order it reproduces the well known Balitsky, Fadin, Kuraev, Lipatov (BFKL) equation [8] and the full equation should be able to resum multiple reggeon exchanges in the structure functions. The crucial assumption which we have to keep in mind is that the series of classical emissions in both nuclei provide us with a set of color charge sources, which give rise to the color field of the produced gluons. This is illustrated in Fig. 1. The QCD evolution, which consists of real terms (classical emissions) and virtual corrections provide us with the color sources, which are denoted by crosses in Fig. 1.

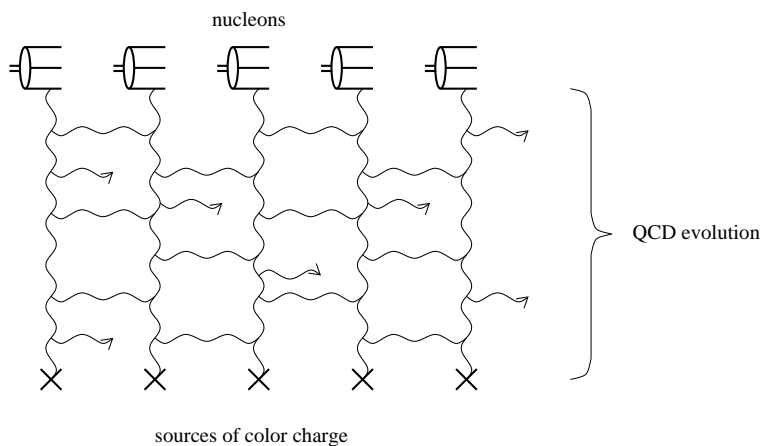


FIG. 1. An example of generation of color charge sources through the QCD evolution in a nucleus. The multiple reggeon evolution, which is described in the text, after a number of iterations, that also include emissions of gluons, produces a number of sea gluons in the rapidity region far away from the nucleus, which later on act as sources of color charge for classical gluon field. The sources are denoted by crosses.

To construct the classical field one has to solve Yang–Mills equations treating the color charges generated through evolution of Fig. 1 in both nuclei as contributions to the source term in the equation. For the field to be purely classical the generated color sources should be separated by the rapidity interval $\delta y \leq 1/\alpha_s$. An example of the diagram contributing to the classical field generated this way is given in Fig. 2. The classical field of colliding nuclei corresponds to gluon production in the approximation, where one resums all powers of the parameter $\alpha_s^2 L$ [3], where L is the number of sources at a given impact parameter. If the total rapidity interval between the colliding nuclei is not very large, $Y \sim 1/\alpha_s$, so that the quantum evolution has not become important yet, the valence quarks in the nucleons will be the sources of color charge and the

resummation parameter will become $\alpha_s^2 A^{1/3}$ [3]. One would have the nucleons instead of the crosses in Fig. 2. Finding the classical field even for this somewhat simplified situation appears to be a complicated task. The problem has been solved analytically only for the gluon production in the case of a proton scattering on a nucleus in [9]. Several attempts have been made for the case of gluon production in nucleus–nucleus collisions [4], giving only the lowest order in α_s result. There have also been done extensive numerical studies of the nucleus–nucleus collisions [10]. In this paper we will not be interested in the detailed structure of the field. What will be important to us is the fact that the classical field is boost invariant, and, therefore, is rapidity independent. Thus if one fixes the configuration of sources in Fig. 2 the classical field in the rapidity interval $\Delta y \sim 1/\alpha_s$ would give rise to a rapidity independent distribution of the produced particles within this rapidity interval.

The classical gluon field has another interesting property. In the regime when the number of color sources is large, making the resummation parameter sizeable, $\alpha_s^2 L \sim 1$, the classical field of Fig. 2 becomes strong, $A_\mu \sim 1/g$ [2,3,7,9]. Since gluons are massless bosons and the typical phase space density is large, we expect that the gluon distribution function at momentum scales less than Λ will saturate with occupation number [2–7,9–15]

$$\frac{1}{\pi R^2} \frac{dN}{d^2 p_T dy} \sim 1/\alpha_s. \quad (5)$$

That way the field is very strong and non-perturbative, even though it could be obtained in the weak coupling regime by usual perturbative methods. The corresponding multiplicities are large [Eq. (5)].

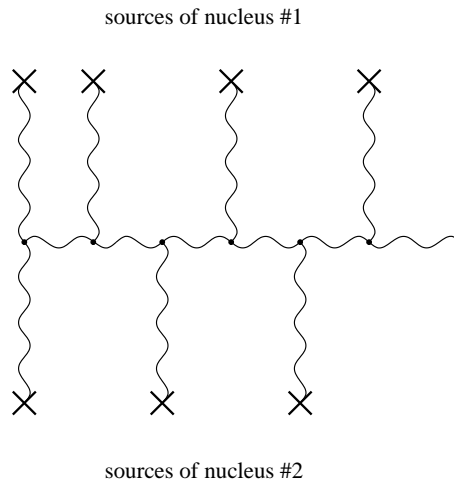


FIG. 2. A classical gluon field produced in a nuclear collision as envisaged in the text. Through QCD evolution nucleons in nuclei give rise to color charge sources (partons) denoted by crosses (see Fig. 1). The sources interact with each other to produce the gluon field.

If the field is classical in each collision, the produced particles arise from a fixed source on an event by event basis. Each event is characterized by a certain configuration of the color charges in the source, off which the classical field of Fig. 2 is emitted. The source results from the fluctuations in the color charge density of those quarks and gluons at rapidities larger or smaller than that at which we measure the distribution of produced particles. We know that the spectrum of fluctuations is Poissonian for a coherent state corresponding to a fixed source density which produces the field. This is similar to the results of reggeon calculus: after fixing the sources the classical fields might be considered as reggeons independently producing particles (see Fig. 3). The spectrum therefore will be Poissonian [16–26]. Moreover, the classical effective action in a random background field of [5,6] describes both the dynamics of the gluon fields and the fluctuations induced by changing the source strength itself. Therefore using the model of classical emissions [2,3,5,6] we should be able to predict the spectrum of rapidity fluctuations at particle formation time.

The nature of the fluctuations in the source density is complicated by the fact that the source density itself satisfies a renormalization group equation [5,6], and is correlated with what the source would have been at other values of rapidity. One of the purposes of this paper is to disentangle this dependence and

to predict the general form of the multiplicity fluctuation spectrum. In Sect. II we shall show that as a consequence of the renormalization group behavior, the fluctuation spectrum exhibits the Koba, Nielsen, and Olesen (KNO) scaling [28]. The KNO scaling for hadron–hadron collisions states that the probability of producing a given multiplicity of particles N at some given high energy E , which we denote dP/dN , multiplied by the average multiplicity of produced particles at this energy $\overline{N}(E)$ is described at all energies by the same scaling function of $N/\overline{N}(E)$ [28]

$$\overline{N}(E) \frac{dP}{dN} = f(N/\overline{N}(E)), \quad (6)$$

characteristic of given hadron species. That way the energy dependence of the high energy inclusive cross sections comes in only through the average multiplicity of the produced particles $\overline{N}(E)$.

The nature of this scaling is slightly modified in the case of a nucleus since in the nuclear collisions there is another parameter in the problem — atomic number of the nucleus A . Many nucleons in the nucleus enhance multiple interactions, changing the shape of the KNO distribution. In this paper we will for simplicity consider only the collisions of identical nuclei having the same atomic number A . The relative width of the distribution depends on the baryon number of the nucleus, and must scale roughly like $1/\sqrt{A^\delta}$, where δ could be 2/3, 1 or 4/3 depending on the saturation model, as will be discussed below in Sect. II. This scaling arises from the fact that nucleons separated by transverse distances greater than or of the order of a Fermi from one another must act independently. Thus for nuclear collisions we predict that the KNO scaling function will depend on A

$$\overline{N}(E) \frac{dP}{dN} = f(A, N/\overline{N}(E)). \quad (7)$$

We will derive this result in Sect. II. It implies that for a nucleus of fixed size A one should observe KNO scaling, but the scaling function will differ from a nucleus to a nucleus. We will also argue that the form of this distribution is

$$f \sim \exp \left[-const A^\delta (\sqrt{N/\overline{N}(E)} - 1)^2 \right] \quad (8)$$

[see Eq. (21)]. This multiplicity distribution has a width

$$\delta N \sim \overline{N}(E)/\sqrt{A^\delta}. \quad (9)$$

Of course the width δN is parametrically of the order of $\sqrt{A^\delta}$, since, as will be shown in Sect. II, $\overline{N}(E) \sim A^\delta$, but the signal for the KNO form is its dependence on energy through the total multiplicity.

Of course, due to the final state interaction of particles, the number of particles in the final state is not expected to be much changed from the initial conditions. We expect therefore that fluctuations in the total particle multiplicity as a function of rapidity on an event by event basis at the particle formation time should be reflected in the final state distribution of produced particles. This should be true up to at least some number such as α_s times $\sqrt{dN/dy}$. If we look for very rare fluctuations, then such fluctuations in the final state interactions should not obscure a huge initial state fluctuation.

In Sect. III we will derive another feature of the underlying classical dynamics which manifests itself in the two particle distribution function. To compute the two particle distribution, for each event we take the multiplicity in some bin at y_1 and multiply by the multiplicity at another rapidity bin y_2 . If the classical fields are the ones responsible for the distribution of the produced particles, we shall show that at the leading order in A the two particle distribution function factorizes into

$$D(y_1, y_2) = \frac{dN}{dy_1} \frac{dN}{dy_2}. \quad (10)$$

The factorization is demonstrated in Fig. 3. Of course this factorization would happen if the distributions were uncorrelated at rapidities y_1 and y_2 . We shall argue that they are in fact very tightly correlated in Sect. IV by introducing a correlation function which would allow one to disentangle the classical effects from other possible mechanisms of particle production.

The classical field responsible for this distribution is constant over a large rapidity interval. Therefore if we measure the multiplicity fluctuation in a rapidity interval centered around y_1 which is several sigma away from the average, the multiplicity in a neighboring rapidity interval centered around y_2 should be roughly the same multiple sigma fluctuation from the average. This very remarkable correlation is a measure of the classical coherence of the field, and is a direct measure of the underlying strong like dynamics of the gluon field. We shall make this argument firm in Sect. IV by introducing a correlation coefficient at a fixed impact parameter of the nuclei $\mathcal{C}(b, y_1, y_2)$ in Eq. (32). The coefficient $\mathcal{C}(b, y_1, y_2)$ is an experimentally measurable observable which is equal to 1 when the particle productions at the rapidities y_1 and y_2 are correlated on the event-by-event basis, and is less than one otherwise. We will argue that if the classical picture of emissions is true this correlation coefficient should be 1 over large intervals in rapidity, $|y_1 - y_2| \sim 1/\alpha_s$. It should fall off for wider rapidity intervals. This prediction could be checked experimentally at RHIC and LHC.

In Sect. IV we also discuss the differences and similarities of the results of our classical approach and the conclusions for rapidity correlations which could be driven out of the old reggeon theory.

We summarize our results in Sect. V.

II. NATURE OF KNO SCALING

In this section, we will study the fluctuation spectra of produced particles. Strictly speaking, we are studying the fluctuation spectrum of produced gluons in early stages of the collisions. The number of gluons is of course modified by subsequent interactions with other gluons and in their subsequent transmutation into pions. It is expected nevertheless that the number of produced pions is close to the number of initially produced gluons. This is because the gluons are thermalized largely by two body collisions in the early stage of the collision, since the coupling is weak if the typical transverse momentum of the gluons is large. This is expected if the multiplicity per unit area Λ^2 of Eq. (3) is large compared to Λ_{QCD}^2 as should be the case for large nuclei at asymptotically high energy. The two body collisions change the transverse momentum distribution of gluons, but preserve the total gluon number. In this paper we are interested in the multiplicities of gluons integrated over all transverse momenta (or coordinates), which do not change under thermalizing two gluon collisions. At later times after thermalization, we expect that entropy will be approximately conserved. At late stages, the entropy is converted into pion number as the system cools. We expect therefore that $dN_{gluon}/dy \sim dN_{pion}/dy$. In general there may be some weak dependence of this proportionality upon multiplicity, but for our purposes this weak dependence will not be important.

Therefore, although we compute the initial multiplicity fluctuations in gluons, this should be reflected in the multiplicity fluctuations of produced pions.

In the McLerran-Venugopalan model of the small x hadronic wave function, one computes a classical field which arises from a source density [2,5]. This source density is at rapidities much larger than that of the classical field which we compute. Eventually the source density is itself integrated over to be included in the source for the next series of classical emissions [5,6], as was described in the introduction.

Let us first compute the fluctuation spectrum of produced particles for a fixed source. In this case, the wavefunction corresponding to this classical field is a coherent state. Coherent state wavefunction generate Poisson distribution in multiplicities. Therefore the typical fluctuation scale in a unit of rapidity is of order $\sqrt{dN/dy}$. We will soon see that this scale is small compared to that generated by the fluctuations in the source itself.

To understand the fluctuations induced by the source of the classical fields, we construct a model which has most of the features of BFKL evolution and fluctuations in the source density. We use intuition developed from understanding the renormalization group structure of the McLerran-Venugopalan model. We use the equation

$$\frac{dN}{dy} = \kappa N(y) + \sqrt{\kappa' N(y)} \zeta(y). \quad (11)$$

In this equation, $N(y)$ is the total number of particles in the rapidity range between y_{target} and y ,

$$N(y) = \int_{y_{target}}^y dy' \frac{dN}{dy'}. \quad (12)$$

The first term on the right hand side of the evolution equation (11) is the toy model analog of the kernel of the BFKL evolution equation (thus $\kappa = \alpha_P - 1 = \frac{4\alpha_s N_c \ln 2}{\pi}$ is the intercept of the BFKL pomeron [8]). For a series of classical emissions one could conclude that the number of produced particles is proportional to the total number of partons off which the new particles are emitted. This is reflected in the first terms of Eq. (11). We note that due to the classical emission picture we can write Eq. (11) for particle multiplicities and not just for the cross sections (The BFKL equation was originally written for the cross section.). The reason for that stems from the fact that at the high energies considered here the total cross sections become independent of energies, thus making the energy dependence of inclusive cross sections and multiplicities identical. If we ignore the second term on the right hand side of Eq. (11) the solution of the equation would be

$$\frac{dN}{dy} = N_0 e^{\kappa(y-y_{target})}, \quad (13)$$

which is our analog of the solution of the BFKL equation. Comparing Eq. (13) to the usual one BFKL pomeron exchange result [8] we note here that $N_0 \sim \alpha_s^2$. The A -dependence of N_0 is determined from the predictions for multiplicity inside of the saturation region. All saturation models [2,15,29] agree that the multiplicity of the produced particles in the saturation region is given by

$$\frac{dN}{dy} \sim A^{2/3} Q_s^2(y) \quad (14)$$

with $Q_s(y)$ the saturation momentum, which is denoted by Λ in Eq. (3). The factor of $A^{2/3}$ in Eq. (14) results from the integration over the impact parameters of the nuclei. In the Glauber–Mueller–type saturation models [30] the saturation momentum scales as $Q_s^2 \sim A^{1/3}$ due to multiple rescatterings within the nucleus. In the approaches based on the BFKL equation [2,29,31] $Q_s^2 \sim A^{2/3}$. In the Reggeon approach [16–26] Q_s^2 is independent of A . We can summarize all these results by writing $N_0 \sim A^\delta$, with δ being dependent on the particular model at hand. In Glauber–Mueller model $\delta = 1$, in BFKL-based approaches $\delta = 4/3$ and in Reggeon calculus $\delta = 2/3$.

The second term on the right hand side of Eq. (11) is stochastic and in our model describes the fluctuations induced at each stage of the evolution equation. The probability distribution of the fluctuation of the stochastic term ζ is Gaussian

$$Z = \int [d\zeta] e^{-\frac{1}{2} \int dy \zeta^2(y)}. \quad (15)$$

Its origin is from the renormalization group [5]. At each step a classical field is induced, which when small fluctuations are computed gets converted into a source for the next step in the evolution. Of course the classical field itself has Poissonian fluctuations which near the center of the distribution should be Gaussian. Therefore, the induces source at the next step will have fluctuations built in which are correlated with the fluctuations in the previous step. If we look over an interval of unit width in rapidity, the weight of these fluctuations is of order $\sqrt{dN/dy}$. Our stochastic source ζ is weighted by the function Z of Eq. (15) so that its fluctuations in one unit of rapidity are also of order one. Using the fact that $\kappa N \sim dN/dy$ which is true for the solution (13) of Eq. (11) without the stochastic term, and, as we shall see below, is approximately valid for the full Eq. (11), we can replace the weight of the stochastic fluctuation term by $\sqrt{dN/dy} \rightarrow \sqrt{\kappa' N}$ arriving at the evolution equation (11). We also note that $\kappa' \sim \alpha_s$.

The solution to Eq. (11) for fixed ζ is

$$N(y) = \left[\sqrt{\overline{N}(y)} + \frac{1}{2} \sqrt{\kappa'} \int_0^y dy' e^{\kappa(y-y')/2} \zeta(y') \right]^2. \quad (16)$$

In Eq. (16)

$$\overline{N}(y) = e^{\kappa y} N_0 \quad (17)$$

where we will in the future set $y_{target} = 0$. Note that \overline{N} is the typical average multiplicity at fixed y which one would have in the limit when fluctuations are turned off.

We can now compute the multiplicity distribution function dP/dN . To this we must integrate over the fluctuations fields ζ with the constraint that the total multiplicity is given by Eq. (16). We have

$$\frac{dP}{dN} = \frac{1}{Z} \int [d\zeta] \exp \left[-\frac{1}{2} \int dy' \zeta^2(y') \right] \delta \left(N(y) - \left[\sqrt{\overline{N}(y)} - \frac{\sqrt{\kappa'}}{2} \int_0^\infty dy' e^{\kappa(y-y')/2} \zeta(y') \right]^2 \right) \quad (18)$$

In this integral, we replaced the upper limit of integration in the expression for $N(y)$ by infinity, since we are typically interested in large values of y . This makes the analysis simpler in what follows.

To evaluate the path integral, one should decompose

$$\zeta(y) = \sum_{n=0}^{\infty} e^{-\kappa y/2} c_n L_n(\kappa y), \quad (19)$$

where the L_n 's are Laguerre polynomials L_n^0 . Using the orthogonality condition for Laguerre polynomials one can see that all the integrals over c_n 's in Eq. (18) become Gaussian with the exception of the integral over c_0 in the numerator, which is fixed by the delta function. The integrals over c_n 's for $n \geq 1$ can be done in closed form and are canceled by the same integrals in Z in the denominator. The final answer is given by the c_0 integration.

In the end, we find that

$$\overline{N}(y) \frac{dP}{dN} = \sqrt{\frac{\kappa N_0 \overline{N}(y)}{2\pi \kappa' N}} \exp \left[-2 \frac{\kappa N_0}{\kappa'} \left(1 - \sqrt{\frac{N}{\overline{N}(y)}} \right)^2 \right]. \quad (20)$$

The multiplicity of the produced particles N_0 is very large. That allows us to expand Eq. (20) around $N = \overline{N}$. We obtain

$$\overline{N}(y) \frac{dP}{dN} = \sqrt{\frac{\kappa N_0}{2\pi \kappa'}} \exp \left[-\frac{\kappa N_0}{2\kappa'} \left(1 - \frac{N}{\overline{N}(y)} \right)^2 \right]. \quad (21)$$

This result for the multiplicity distribution is simple to understand. The evolution equation connects the produced particle to some initial spectrum of fluctuations. The relative importance of these fluctuations decreases as the multiplicity increases. Therefore the fluctuations within an interval of width $1/\alpha_s$ in rapidity set up the fluctuations at higher values. This is the factor of $\kappa N_0/\kappa'$ in the exponent of Eq. (21). Remembering that $\kappa \sim \kappa' \sim \alpha_s$ and $N_0 \sim \alpha_s^2 A^\delta$ we conclude that the relative width of the multiplicity distribution scales like $1/\alpha_s \sqrt{A^\delta}$. The fluctuations are all correlated all the way down the chain and therefore should only depend upon the ratio $N/\overline{N}(y)$. This dependence is the essence of KNO scaling. The only important variable is the multiplicity divided by the average multiplicity. Of course there is also a dependence on N_0 because there are more independent emitters for a nucleus than for a hadron. This is reflected in the fact that $N_0 \sim A^\delta$.

Note that the width of this distribution is

$$\delta N^2 \sim \overline{N}^2(y) \kappa' / N_0 \kappa. \quad (22)$$

Parametrically δN^2 is linear in A^δ , as $N_0 \sim A^\delta$ and $\overline{N} \sim N_0 \sim A^\delta$.

In general, the fluctuation spectrum for the first few emitters which generate the fluctuations in the distribution may be different from Eq. (21). The exact shape of the KNO scaling function will probably differ from the one given by Eqs. (20) and (21). Nevertheless, the physical picture we have generated still is true, and therefore we expect that in general the distribution will be of the form

$$\overline{N}(y) \frac{dP}{dN} = f(N_0, N/\overline{N}(y)) \quad (23)$$

and that the typical width of the distribution will scale with A and α_s in the same way as the width in our model given by Eq. (22). The physical picture we have of the small x gluon distribution functions therefore automatically has KNO scaling [cf. [13]].

In terms of the strong coupling constant the relative width $\delta N^2/\overline{N}^2(y) \sim 1/\alpha_s^2$ (see Eq. (22)). It has been argued in the framework of McLerran–Venugopalan model that in high energy nuclear scatterings the high parton density sets the scale of the running coupling constant [2,5,6]. If this assumption is true, than one could conclude that at very high energies $N_0 \sim \alpha_s^2(\Lambda_{target})$, since N_0 is the multiplicity of the particles in the fragmentation region. Λ_{target} is the transverse momentum scale characterizing the target nucleus. At the same time $\kappa \sim \alpha_s(\Lambda)$, as it determines the evolution of the multiplicity $N(y)$ at some large rapidity y . (Λ is given by Eq. (3).) κ' depends on y through its dependence on $\Lambda \sim N(y)$. However, if we allow κ' to depend on y then, since the integral over y' in Eq. (16) is dominated by $y' \approx 0$ one can see that the most important value of κ' would be at the fragmentation region. Thus $\kappa' \sim \alpha_s(\Lambda_{target})$. In the light of the above estimates and using Eq. (22) we conclude that the relative width depends on the average multiplicity

$$\frac{\delta N^2}{\overline{N}^2(y)} \sim \frac{1}{\alpha_s(\Lambda) \alpha_s(\Lambda_{target})} \sim \frac{1}{\alpha_s(N)}. \quad (24)$$

The high multiplicity of the produced particles would create a large momentum scale Λ , which would make the coupling constant $\alpha_s(\Lambda)$ small. Thus the relative width of the KNO distribution given by Eq. (24) will get larger. Moreover, since the change in width would depend on the average multiplicity of the produced particles that would violate the KNO scaling. Thus our prediction of KNO scaling will start to break down slowly at very high energies. At the same time since the rate of change of the running coupling constant $\alpha_s(\Lambda)$ slows down at large Λ the violation of KNO scaling will decrease as the energy gets higher.

III. CLASSICAL NATURE OF THE DISTRIBUTION FUNCTION

Another feature of the classical field particle production arises from considering the distribution function $D(y_1, y_2)$. We define this to be the two particle distribution function measured in the following way: In each event or class of events, measure the multiplicity of particles at rapidities y_1 and y_2 in bins of width dy_1 and dy_2 . Multiply these multiplicities together to generate

$$d^2 N(y_1, y_2) = D(y_1, y_2) dy_1 dy_2. \quad (25)$$

Then average $D(y_1, y_2)$ over events or classes of events.

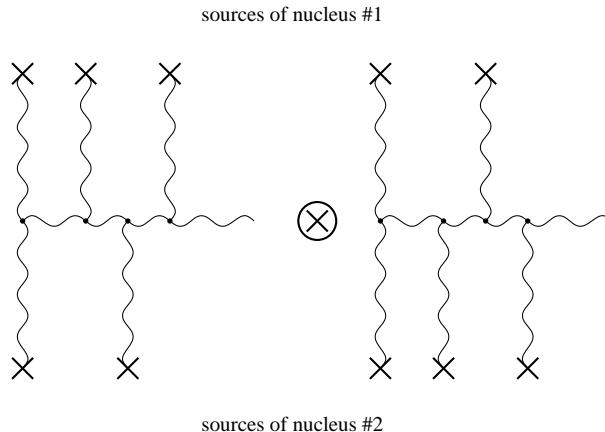


FIG. 3. Classical production of two gluons in nuclear collision as described in the text. The figure illustrates factorization of Eq. (28).

A class of events might be generated by putting a cut on say the total multiplicity of particles in the neighborhood of zero rapidity. In the class of events where this cut is satisfied, one could measure the multiplicity in different regions of rapidity and average over the class of events.

The distribution function D may be generated as an expectation value of the number operator

$$D(y_1, y_2) = \int \frac{d^2 p_T}{(2\pi)^2} \frac{d^2 q_T}{(2\pi)^2} \langle a^\dagger(y_1, p_T) a(y_1, p_T) a^\dagger(y_2, q_T) a(y_2, q_T) \rangle. \quad (26)$$

In the classical field limit, this expression is of the form

$$\langle a^\dagger(y_1, p_T) a(y_1, p_T) a^\dagger(y_2, q_T) a(y_2, q_T) \rangle \sim A^i(p) A^i(-p) A^i(q) A^i(-q) \quad (27)$$

where A^i is the classical field produced by the color sources in the colliding nuclei [4,9,10]. When one averages over the sources which generate the fields, one finds that

$$D(y_1, y_2) = \left\langle \frac{dN}{dy_1} \right\rangle \left\langle \frac{dN}{dy_2} \right\rangle. \quad (28)$$

This is true up to corrections which are of order $A^{-2/3}$, that is of the order of one over the area of the nuclei. This statement could be understood from Fig. 3. The classical fields producing the gluon connect to several color sources. In the leading order in A the fields generating gluons at y_1 and y_2 connect to different sets of color sources, making Eq. (28) true.

Note that this tells us that the fields are essentially trivially correlated in the longitudinal direction. The connected piece of $D(y_1, y_2)$ has vanished entirely, up to corrections which go like one over the area of the nuclei. This lack of correlation is not by itself evidence of a classical field. It could occur if there were for example no correlations at all in the longitudinal space. The structure of the KNO distribution itself suggests that this is not the case. In the next section, we shall see that there is a correlation function which dramatically illustrates the classical correlation.

IV. CLASSICAL CORRELATION

If there are classical fields, then, as we have seen above, due to boost invariance, these classical fields are independent of rapidity over a wide range of rapidity [4,9]. Therefore the multiplicity should on the average be the same over the range of rapidity where the classical field theory is valid. This is typically of order $1/\alpha_s$ in the classical field approach. At the same time α_s should be small when the density of produced particles is large [2], making this correlation length in rapidity large.

This effect can be measured in the following way: Measure the rapidity density in some bin of width dy_1 around y_1 and dy_2 around y_2 . Require that dy_1 and dy_2 are large enough so that the statistical fluctuations in the rapidity in a given event are small compared to the total multiplicity. From our picture of classical particle production it follows that the multiplicity around y_1 should be the same as around y_2 up to statistical fluctuations.

If we applied this analysis to an average event, the result above would be trivial. On the other hand, if we look at an event where the fluctuation is very rare in the bin around y_1 , we predict that there will also be the same rare fluctuations around y_2 ! Rare events tend to fluctuate together over a wide range of rapidity!

A measurement of the width of the correlation length tells us something about the underlying classical dynamics and is interesting in itself.

First we note that in a nuclear collision $\frac{dN}{dy}$ is a function of rapidity y , impact parameter of the nuclei b , and of the configuration of color charges in the nuclei in this particular collision, which we will symbolically denote ρ :

$$\frac{dN}{dy} = \frac{dN}{dy}(y, b, \rho). \quad (29)$$

If one measures $\frac{dN}{dy}$ in a number of events and then takes the average value at a fixed impact parameter of the colliding nuclei b the result should correspond to the averaging of the theoretical prediction for $\frac{dN}{dy}$ over all configurations of color charges in the colliding nuclei ρ , which we write as

$$\left\langle \frac{dN}{dy}(y, b, \rho) \right\rangle_\rho. \quad (30)$$

Event by event fluctuations in $\frac{dN}{dy}(y, b, \rho)$ are characterized by the variance of that quantity which we will define as

$$V \left[\frac{dN}{dy} \right] = \left\langle \left(\frac{dN}{dy}(y, b, \rho) \right)^2 \right\rangle_{\rho} - \left\langle \frac{dN}{dy}(y, b, \rho) \right\rangle_{\rho}^2. \quad (31)$$

Thus we can also introduce the correlation function of the numbers of particles measured at two different rapidity points y_1 and y_2 in several events with the same impact parameter (that is for several configurations of color charges ρ). According to the standard mathematical methods we define the correlation coefficient

$$\mathcal{C}(b; y_1, y_2) = \frac{\left\langle \frac{dN}{dy_1 dy_2}(b, \rho) \right\rangle_{\rho} - \left\langle \frac{dN}{dy_1}(b, \rho) \right\rangle_{\rho} \left\langle \frac{dN}{dy_2}(b, \rho) \right\rangle_{\rho}}{\sqrt{V \left[\frac{dN}{dy_1} \right] V \left[\frac{dN}{dy_2} \right]}}. \quad (32)$$

We can neglect the y dependence of $\frac{dN}{dy}(y, b, \rho)$ for the rapidity intervals of the size $1/\alpha$. That way one can see that when $|y_1 - y_2| \lesssim 1/\alpha$ we can neglect the variation of $\frac{dN}{dy}(b, \rho)$ with y , which is purely statistical in that interval, and put $\frac{dN}{dy_1} \approx \frac{dN}{dy_2}$, which leads to $\mathcal{C}(b; y_1, y_2) = 1$. This is the prediction of the classical emission picture discussed above and in [2,3]: the correlation function $\mathcal{C}(b; y_1, y_2)$ should be close to one for $|y_1 - y_2| \lesssim 1/\alpha$. When $|y_1 - y_2| \gtrsim 1/\alpha$ the y dependence in $\frac{dN}{dy}$ in the interval between y_1 and y_2 becomes important and $\frac{dN}{dy_1}$ and $\frac{dN}{dy_2}$ become uncorrelated, which would lead to $\mathcal{C}(b; y_1, y_2)$ being smaller than one.

One might note that in the leading powers of A approximation both numerator and denominator in the expression for $\mathcal{C}(b; y_1, y_2)$ given by Eq. (32) are zero. The non-zero terms appear once we include the corrections which are subleading in A . The first non-zero terms in the numerator and denominator of Eq. (32) are suppressed by $A^{2/3}$ compared to the leading contribution in, for instance, $\frac{dN}{dy_1 dy_2}(b, \rho)$. That is if we calculate $\frac{dN}{dy_1 dy_2}(b, \rho)$ in the classical approximation we would obtain the leading term in A given by Eq. (28), which is canceled in the numerator of Eq. (32), and the subleading terms, which are suppressed at least by $A^{2/3}$, but still arise from the classical approximation. The largest of these subleading terms is suppressed by exactly $A^{2/3}$ and results from the situation when both particles at y_1 and y_2 are emitted from the same nucleon. Even though it is subleading in A this term is nevertheless larger than the correlations induce by quantum corrections connecting the fields that produce the particles at y_1 and y_2 , since the latter are also suppressed by extra powers of α_s . The quantum correction within one of the fields do not violate the factorization of Eq. (28) and, therefore, cancel in the numerator of Eq. (32). Thus the fact that the correlator in Eq. (32) is equal to 1 because of the terms in the numerator and denominator which are subleading in A does not influence the fact that the correlations are classical.

In order to understand Eq. (32) better let us consider different possible definitions of the correlation function. For rapidity correlation function defined as

$$\mathcal{R}_{\rho}(y_1, y_2) = \frac{\frac{dN}{dy_1 dy_2}(b, \rho) - \frac{dN}{dy_1}(b, \rho) \frac{dN}{dy_2}(b, \rho)}{\frac{dN}{dy_1}(b, \rho) \frac{dN}{dy_2}(b, \rho)} \quad (33)$$

we expect that

$$\mathcal{R}_{\rho}(y_1, y_2) = O\left(A^{-\frac{2}{3}}\right). \quad (34)$$

Note, that in Eq.(32) we fix the value of the impact parameter (transverse distance between centers of colliding nuclei) which is also a characteristics of the event. The $A^{-\frac{2}{3}}$ - corrections stem from region of integration $p_T \approx q_T$ in Eq. (27). This is the subleading correction to the factorization of Eq. (28). It could also be viewed as resulting from the contribution when the two fields of Fig. 3 share the same source of color charge. That term would definitely be suppressed by $A^{2/3}$. Thus the correlation coefficient of Eq. (33) defined without averaging over events does not reflect the correlations that we are interested in. However, R_{ρ} is not the correlation coefficient usually employed in the experiments. One defines the correlation function $\mathcal{R}_{average}$ by

$$\mathcal{R}_{average}(y_1, y_2) = \frac{\frac{1}{\sigma_{tot}} \left\langle \frac{d\sigma}{dy_1 dy_2} \right\rangle_{b,\rho} - \frac{1}{\sigma_{tot}} \left\langle \frac{d\sigma}{dy_1} \right\rangle_{b,\rho} \frac{1}{\sigma_{tot}} \left\langle \frac{d\sigma}{dy_2} \right\rangle_{b,\rho}}{\frac{1}{\sigma_{tot}} \left\langle \frac{d\sigma}{dy_1} \right\rangle_{b,\rho} \frac{1}{\sigma_{tot}} \left\langle \frac{d\sigma}{dy_2} \right\rangle_{b,\rho}} \quad (35)$$

where σ_{tot} , $\frac{d\sigma}{dy}$ and $\frac{d\sigma}{dy_1 dy_2}$ are total, single and double inclusive cross sections for nuclear collisions that are defined by averaging over all events (ρ) and integrating over all impact parameters (b_t). As was shown long ago in the Pomeron approach function $\mathcal{R}_{average}$ generally is of the order of unity even in the case if have $\mathcal{R}_\rho = 0$ [16]. However, we would like to point out that the main correlation which makes $\mathcal{R}_{average}$ large is the simple correlation in impact parameters which has a very simple underlying physics, which states that partons (gluons) are produced independently but at the same value of impact parameter. In McLerran-Venugopalan model one might expect that at high parton densities or better to say in collisions of heavy nuclei the b_t - distribution for all physical observables are the same, namely, $\Theta(R_A - b_t)$. In this case $\mathcal{R}_{average} \rightarrow 0$ showing a classical field emission even without the event selection (b_t fixing). If one does not integrate over the impact parameter in Eq. (35) then without the impact parameter correlations this correlation function will be small again failing to reflect the type of correlations we are interested in.

The general picture of correlations for high parton density QCD turns out to be very similar to pattern of correlations predicted by the Reggeon approach which has been discussed in details for three decades [16–27]. The first observation is that in both approaches Eqs. (27) and (33) lead to conclusion that the secondary gluons (hadrons) are originated from the independent production of clusters with the mean multiplicity $\langle N \rangle = \int \frac{dN}{dy}(y, \rho, b_t) dy$. Therefore, the probability to emit $k \times \langle N \rangle$ gluons or, in other words, k clusters, is equal to

$$P_k = e^{-\langle N \rangle} \frac{\langle N \rangle^k}{k!}. \quad (36)$$

Note, that Eq. (36) is a well known Poisson distribution.

The second observation stems from the classical field emission, namely, $\frac{dN}{dy}(y, \rho, b_t) = d = Const(y) \gg 1$ for the rapidity interval of the order of $1/\alpha_s \gg 1$. We will discuss why $d \gg 1$ below. Assuming this we can easily see that we can neglect statistic fluctuations in $N(y, \rho, b_t)$, and, therefore, $\langle N \rangle = Y d$ where Y is the accessible rapidity interval ($Y \propto 1/\alpha_s$). We can claim even that $N(y, \rho, b_t)$ which is defined as the number of gluons (hadrons) in the rapidity interval $y - \Delta y \div y + \Delta y$ is equal to

$$N(y, \rho, b_t) = k \times d \times 2\Delta y. \quad (37)$$

Therefore, measuring $N(y, \rho, b_t)$ we fix the number of clusters k or, in other words, we select a configuration which is produced with probability P_k (see Eq. (36)).

Let us recall the main predictions that will hold both in classical field approach (McLerran-Venugopalan model) and in the Reggeon description. If we select the events where the multiplicity of the particles in the rapidity bin $y_1 - \Delta y \div y_1 + \Delta y$ around y_1 ($N(y_1)$) is fixed and average the multiplicity in the rapidity interval $y_2 - \Delta y \div y_2 + \Delta y$ over these events we predict that it will be equal to

$$\langle N(y_2) \rangle_{N(y_1) fixed} = N(y_1). \quad (38)$$

Also the number of neutral pions in rapidity interval $y_1 - \Delta y \div y_1 + \Delta y$ ($N_0(y_1)$) averaged over the events with a fixed number of charged pions in the same bin should be equal to

$$\langle N_0(y_1) \rangle_{N^{ch}(y_1) fixed} = \frac{1}{2} N^{ch}(y_1), \quad (39)$$

where $N^{ch}(y_1)$ is the number of charged pions. Both models predict that for heavy ion-ion collisions in the kinematic region of saturation [2,15] we have

$$\mathcal{R}_{average}(y_1, y_2) \rightarrow 0 \left(\frac{1}{A^{2/3}} \right). \quad (40)$$

One can see that all these prediction are direct consequences of Eq. (36) and Eq. (37). Much more detailed predictions could be found in Refs. [17–27].

The high density QCD and soft Reggeon approaches can be distinguished by measuring the transverse momenta distributions or/and transverse momenta correlation between produced particles. Indeed, in high parton density QCD the typical transverse momentum of produced gluons (saturation momentum $Q_s(A, x)$) is large and depends on A [2,15] while in the Reggeon approach this momentum is constant and rather small — about 2 GeV, which results from the slope estimates of the soft pomeron. However, at first sight, this main difference does not influence the shape of the rapidity correlations and only increases the multiplicity of produced particles making our predictions more reliable in this case. Indeed, the saturation of the gluon density leads to $d \propto Q_s^2(W, A)$ [2,3,5,15,29,31] where W is the energy in the center of mass frame and $Q_s^2(W, A)$ is the saturation scale Eq. (14), which is similar to Λ of Eq. (3). Since $Q_s^2(W, A)$ increases with W and A (at least $Q_s^2 \propto A^{\frac{1}{3}}$ [2,3,5,15,29] but it could even be proportional to $A^{\frac{2}{3}}$ [31]) we expect $d \gg 1$ which makes all of our estimates much more accurate than the results of the Reggeon approach [22] [32]. As far as the shape of the rapidity correlations is concerned the saturation of the parton densities [2,3,5,15,29,31] leads to sufficiently large correlation length which is proportional to $1/\alpha_s(Q_s)$. For heavy nuclei and/or high energies Q_s increases and $\alpha_s \rightarrow 0$. This fact leads to Eq. (37) being better justified in the high parton density QCD than in the case of the Reggeon approach.

V. CONCLUSIONS

In this paper we have considered the consequences of the model of classical emissions on the particle production mechanisms in heavy ion collisions [2]. We have argued that the classical fields do not vary significantly over the rapidity intervals of the order of $1/\alpha_s$. This led us to conclude that the multiplicities of the particles produced in the early stages of the collisions (gluons) are correlated over $1/\alpha_s$ units of rapidity on the event-by-event basis. We then gave an argument demonstrating that the number of gluons generated in a particular collision is proportional to the number of pions produced in the final state. Therefore the correlation in the multiplicities of the produced gluons would reflect themselves in the multiplicities of the final state pions. We have then constructed the correlation function $\mathcal{C}(b; y_1, y_2)$ in Eq. (32), which could be measured experimentally and is equal to 1 when the multiplicities of particles at the rapidities y_1 and y_2 are correlated and is less than 1 otherwise. Surprisingly this effect comes from the terms in the numerator and denominator of the expression for $\mathcal{C}(b; y_1, y_2)$ given by Eq. (32) which are subleading in A . We predict $\mathcal{C}(b; y_1, y_2)$ to be close to 1 when $|y_1 - y_2| \leq 1/\alpha_s$ and fall off for larger rapidity intervals.

We have also used the model of classical particle production to explain KNO scaling. In a simple toy model which resulted from trying to mimic the main features of the classical emissions we have reproduced KNO scaling for the multiplicities of produced particles. The result is given in Eq. (21). Even though the exact shape of the KNO distribution function is, probably, different from our toy model prediction, we believe that the model captures its main features. For the case of nuclei we predict the KNO function to depend on the atomic number A in addition to the usual dependence on $N/\bar{N}(y)$. We predict that at very high energies KNO scaling in nuclear collisions will be violated due to the running of the coupling constant, which would get smaller as parton density increases.

The main results of this paper can be summarized in the following way:

1. We have derived KNO scaling from the classical emission picture of particle production (see Eqs. (20) and (21)).
2. We predict rapidity correlations on the scales $\delta y \sim 1/\alpha_s$ in the particle (pion) production in heavy ion collisions on the event-by-event basis (Sect. IV).
3. We proposed a correlation coefficient $\mathcal{C}(b; y_1, y_2)$ which would allow one to measure the predicted correlations (see Eq. (32)).

ACKNOWLEDGMENTS

The authors would like to acknowledge helpful and encouraging discussions with Errol Gotsman, Miklos Gyulassy, Jamal Jalilian-Marian, Uri Maor, Al Mueller, Mark Strikman, Kirill Tuchin, Raju Venugopalan,

and Heribert Weigert.

This work was carried out while E.L. was on sabbatical leave at BNL. E.L. wants to thank the nuclear theory group at BNL for their hospitality and support during that time.

The research of E.L. was supported in part by the Israel Science Foundation, founded by the Israeli Academy of Science and Humanities.

This research has been supported in part by the joint American–Israeli BSF Grant # 9800276. This manuscript has been authorized under Contract No. DE-AC02-98CH10886 with the U.S. Department of Energy.

-
- [1] *Last Call for RHIC Predictions*, proceeding of Quark Matter 99, XIV International Conference on Ultra-Relativistic Nucleus-Nucleus Collisions, nucl-th/9907090.
 - [2] L. McLerran and R. Venugopalan, Phys. Rev. **D 49** (1994) 2233; **49** (1994) 3352; **50** (1994) 2225.
 - [3] Yu. V. Kovchegov, Phys. Rev. **D 54** 5463 (1996); **D 55** 5445 (1997).
 - [4] A. Kovner, L. McLerran, and H. Weigert, Phys. Rev. **D52**, 3809 (1995); 6231 (1995); Yu. V. Kovchegov and Dirk H. Rischke, Phys. Rev. **C56**, 1084 (1997).
 - [5] J. Jalilian-Marian, A. Kovner, L. McLerran, and H. Weigert, Phys. Rev. **D 55**, 5414 (1997).
 - [6] J. Jalilian-Marian, A. Kovner, A. Leonidov, and H. Weigert, Nucl. Phys. **B 504**, 415 (1997); Phys. Rev. **D 59** 014014 (1999); J. Jalilian-Marian, A. Kovner, and H. Weigert, Phys. Rev. **D 59** 014015 (1999); J. Jalilian-Marian, A. Kovner, A. Leonidov, and H. Weigert, Phys. Rev. **D59**, 034007 (1999).
 - [7] A. H. Mueller, hep-ph/9906322, hep-ph/9909388.
 - [8] E.A. Kuraev, L.N. Lipatov and V.S. Fadin, *Sov. Phys. JETP* **45**, 199 (1978); Ya.Ya. Balitsky and L.N. Lipatov, *Sov. J. Nucl. Phys.* **28**, 22 (1978).
 - [9] Yu. V. Kovchegov, A.H. Mueller, Nucl. Phys. **B 529**, 451 (1998).
 - [10] A. Krasnitz, R. Venugopalan, Nucl. Phys. **B557**, 237 (1999); hep-ph/9909203.
 - [11] A. H. Mueller, Nucl. Phys. **B415**, 373 (1994).
 - [12] A.H. Mueller and B. Patel, Nucl. Phys. **B425**, 471 (1994).
 - [13] A.H. Mueller, Nucl. Phys. **B437**, 107 (1995).
 - [14] Z. Chen, A.H. Mueller, Nucl. Phys. **B451**, 579 (1995).
 - [15] L. V. Gribov, E. M. Levin, and M. G. Ryskin, Phys. Lett. **B 100**, 173 (1981); Phys. Rep. **100**, 1 (1983).
 - [16] E. M. Levin, M.G. Ryskin and N.N. Nikolaev, Z. Phys. **C5** (1980) 285.
 - [17] A.H. Mueller, Phys. Rev. **D2** (1970) 2963; Phys. Rev. **D4** (1971) 150.
 - [18] O.V. Kancheli, JETP Letters **18** (1973) 274.
 - [19] V.A. Abramovskii, V.N. Gribov and O.V. Kancheli, Sov. J. Nucl. Phys. **18** (1974) 308.
 - [20] E.M. Levin and M. G. Ryskin, JETP Letters **18** (1973) 654;Sov. J. Nucl. Phys. **19** (1974) 669; **20** (1974) 519; **21** (1975) 396.
 - [21] J. Koplik and A.H. Mueller, Phys. Let. **B58** (1975) 166; Phys. Rev. **D12** (1975) 3638.
 - [22] A. Schwimmer, Nucl. Phys. **B94** (1975) 445.
 - [23] A. Capella and A. Krzywicki, Phys. Let. **B67** (1977) 331.
 - [24] A.B. Kaidalov and K. A. Ter Martirosyan, Phys. Let. **B117** (1982) 247; A.B. Kaidalov, K. A. Ter Martirosyan and Yu. M. Shabelsky, Sov. J. Nucl. Phys. **43** (1986) 822.
 - [25] A. Capella, U. Sukhatme, C.-I. Tan and J. Tran Thanh Van, Phys. Report **236** (1994) 225 and references therein.
 - [26] A. Capella, A. Kaidalov and J. Tran Thanh Van, Heavy Ion Phys. **9** (1999) 169 and references therein.
 - [27] G. Baym, B. Blattel, L.L. Frankfurt, H. Heiselberg, and M. Strikman, Phys. Rev. **C 52**, 1604 (1995) and references therein.
 - [28] Z. Koba, H. B. Nielsen, and P. Olesen, Nucl. Phys. **B 40**, 317 (1972).
 - [29] Yu. V. Kovchegov, Phys. Rev. **D 60**, 034008 (1999); hep-ph/9905214.
 - [30] A.H. Mueller, Nucl. Phys. **B335**, 115 (1990).
 - [31] E. Levin and K. Tuchin, hep-ph/9908317.
 - [32] S. Bondarenko, E. Gotsman, E. Levin and U. Maor, in preparation.